

## SUPPORTING INFORMATION

# **Kinetic Optimization of the Batch Crystallization of an Active Pharmaceutical Ingredient in the Presence of a Low-Solubility, Precipitating Impurity**

**Mitchell Paolello <sup>1</sup>, Ilyes Bichari <sup>2</sup>, Davinia Brouckaert <sup>2</sup>, Mirvatte Francis <sup>2</sup>, Dawn Yang <sup>2</sup> and Gerard Capellades <sup>1,\*</sup>**

<sup>1</sup> Department of Chemical Engineering, Rowan University, Glassboro, NJ 08028, United States; capellades@rowan.edu

<sup>2</sup> Indatech, Chauvin Arnoux Group, 34830 Clapiers, France

\* Author to whom correspondence should be addressed

### Raman Spectra for Pure Components

The reference Raman spectra were obtained from pure ACM and pure CUR that were suspended in 25/75 EtOH/H<sub>2</sub>O solvent, which was the solvent composition in which both solids were crystallized. In addition, a spectra was taken for the solvent itself. The reference spectra are all illustrated in Figure S1. The solvent peak at 850 cm<sup>-1</sup> is correlated to the liquid phase concentration of ACM. The peak decreases as ACM liquid concentration increases and as ACM crystallizes out. The PLS model is not affected by an increase or decrease in the peak when ACM increases as it correlates this variability to the liquid concentrations directly.

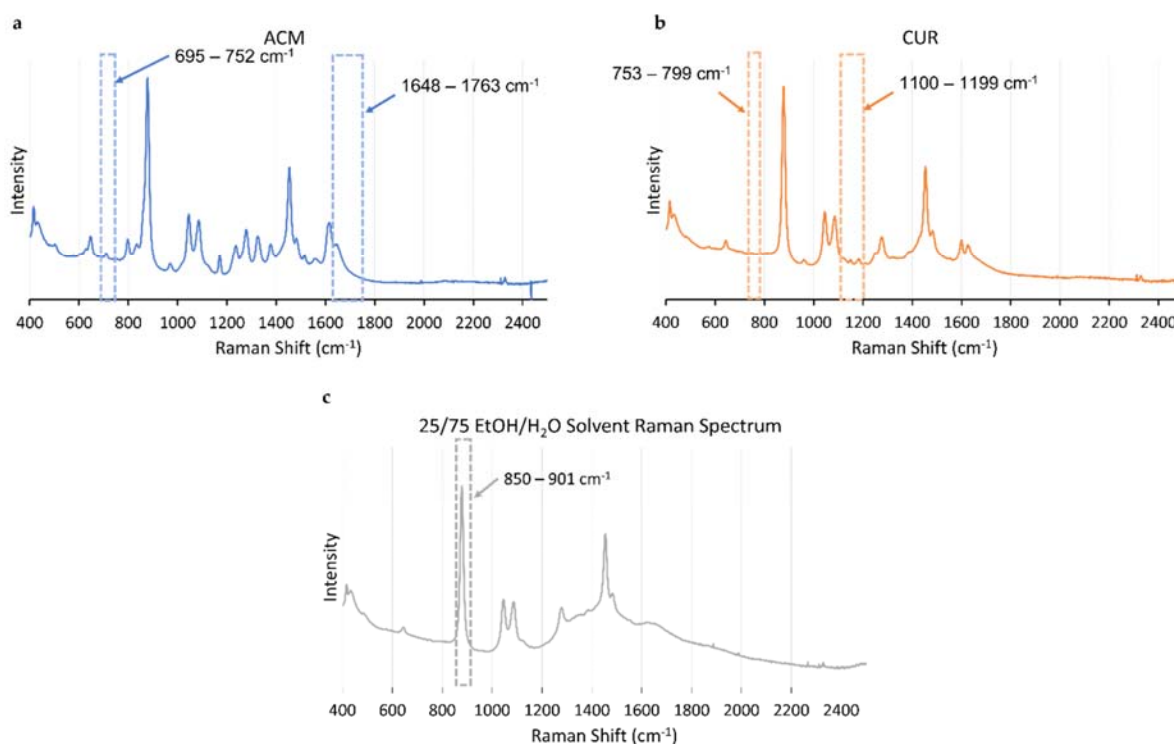


**Figure S1.** Raman spectra for pure ACM (a), pure CUR (b) and the 25/75 EtOH/H<sub>2</sub>O solvent (c).

There is a small band in the solvent spectrum at 1648 cm<sup>-1</sup> (Fig. S1c). A peak is detected at this point in the presence of ACM (Fig. S1a). Although there is a peak for CUR at 1626 cm<sup>-1</sup> (Fig. S1b), CUR is much less concentrated in the liquid phase than ACM and is also close to the ACM peak. The ACM and CUR peaks in this region are dependent on each other since their peaks are closely aligned and have been observed to merge into a single peak. Preprocessing was done as explained in Section 4.1 of the Results to reduce the correlation between the ACM and CUR peaks in this region.

## Particle Size Distributions

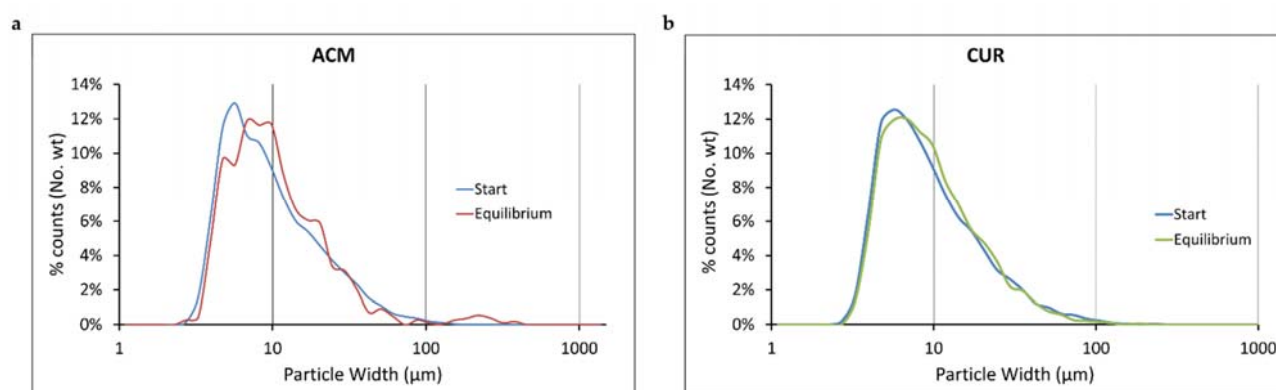


**Figure S2.** Particle width distributions for ACM (a) and CUR (b) indicate little change in the number of small particles between the start of the crystallization and at equilibrium. These observations led to the assumption that secondary nucleation of ACM and CUR is negligible, and the primary kinetic mechanism is growth on the seed crystals.

## **gPROMS Nomenclature for Parameter Estimation Model**

**Table S1.** Model equations for parameter estimation, including equation size for gPROMS FormulatedProducts.

Description	Equation Form	Size
Total Concentrations	$C_{tot,i} = C_c P_{c,i} + C_s P_{s,i}$	NS
Seed Concentrations	$M_{s,i} = C_s P_{s,i}$	NS
Phase Balance	$C_{tot,i} = C_{ml,i} + M_{T,i}$	NS
Supersaturation	$\sigma_i = \ln\left(\frac{C_{ml,i}}{C_{sat,i}}\right)$	NS
Nucleation Rate	$B_i = k_{b,i} M_{T,i}^{j_i} \sigma_i^{b_i}$	NS
Growth Rate	$G_i = k_{g,i} \sigma_i^{g_i}$	NS
Yield, or % Solute Crystallized	$Y_i = \frac{M_{T,i} - M_{s,i}}{C_{tot,i} - M_{s,i}} 100$	NS
% Progress to Equilibrium	$E_i = \frac{M_{T,i} - M_{s,i}}{C_{tot,i} - M_{s,i} - C_{sat,i}} 100$	NS
Product Purity	$P_{p,i} = \frac{M_{T,i}}{\sum_{j=NS} M_{T,j}} 100$	NS
First moment	$\frac{d\mu_{1,i}}{dt} = G_i \mu_{0,i}$	NS
Second moment	$\frac{d\mu_{2,i}}{dt} = 2G_i \mu_{1,i}$	NS
Desupersaturation Rate	$\frac{dC_{ml,i}}{dt} = -3k_{v,i} \rho_i G_i \mu_{2,i} \cdot 10^{-12} \text{ mL}/\mu\text{m}^3$	NS

**Table S2.** Model parameters for the equations in Table S1, as they would be implemented to gPROMS FormulatedProducts.

Symbol	Description	Units	gPROMS Identifier	Size	Type
NS	System solutes	-	solutes	-	ORDERED_SET
$b_i$	Nucleation rate order for supersaturation, solute i	-	b_order	NS	REAL
$g_i$	Growth rate order for supersaturation, solute i	-	g_order	NS	REAL
$j_i$	Nucleation rate order for suspension density, solute i	-	j_order	NS	REAL
$k_{b,i}$	Nucleation rate constant, solute i	#/L/s	nuc_constant	NS	REAL
$k_{g,i}$	Growth rate constant, solute i	$\mu\text{m/s}$	gr_constant	NS	REAL
$k_{v,i}$	Crystal volumetric shape factor, solute i	-	V_shape_factor	NS	REAL
$\rho_i$	Density of the crystalline solute, solute i	g/mL	density	NS	REAL

**Table S3.** Model variables for the equations in Table S1, as they would be implemented to gPROMS FormulatedProducts.

Assigned variables    Supplied during parameter estimation, with initial conditions

Symbol	Description	Units	gPROMS Identifier	Size	Type
$B_i$	Nucleation rate, solute i	$L^{-1} s^{-1}$	rate_nucleation	NS	nucleation_rate
$C_c$	Mass fraction of crude in the starting solution	g/L	crude_conc	-	concentration
$C_{ml,i}$	Mass fraction of solute i in the mother liquor	g/L	ml_conc	NS	concentration
$C_s$	Mass fraction of seeds in the system	g/L	seeds_conc_total	-	concentration
$C_{sat,i}$	Solubility of solute i	g/L	solubility	NS	concentration
$C_{tot,i}$	Mass fraction of solute i in the system	g/L	total_conc	NS	concentration
$E_i$	Percent progress to equilibrium, solute i	%	progress	NS	yield
$G_i$	Linear crystal growth rate, solute i	$\mu m/s$	rate_growth	NS	growth_rate
$M_{s,i}$	Seed solids concentration, solute i	g/L	seeds_conc_component	NS	concentration
$M_{T,i}$	Total solids concentration, solute i	g/L	solids_conc	NS	concentration
$P_{c,i}$	Crude purity for solute i	g/g	crude_purity	NS	mass_fraction_gFP
$P_{p,i}$	Product purity for solute i	%	product_purity	NS	purity
$P_{s,i}$	Seed purity for solute i	g/g	seed_purity	NS	mass_fraction_gFP
$Y_i$	Yield for solute i	%	yield	NS	yield
$\sigma_i$	Supersaturation for solute i	-	supersaturation	NS	supersaturation
$\mu_{0,i}$	zeroth moment solute i	$L^{-1}$	zeroth_moment	NS	zeroth_moment
$\mu_{1,i}$	1st moment solute i	$\mu m/L$	first_moment	NS	first_moment
$\mu_{2,i}$	2nd moment solute i	$\mu m^2/L$	second_moment	NS	second_moment